C. R. Geoscience 351 (2019) 104–112

Contents lists available at ScienceDirect

Comptes Rendus Geoscience

www.sciencedirect.com

Internal Geophysics (Physics of Earth's Interior)

High-pressure and high-temperature stability of chlorite and 23-Å phase in the natural chlorite and synthetic MASH system

Nao Cai [a,*], Toru Inoue [a,b,c]

[a] Geodynamics Research Center, Ehime University, 2-5 Bunkyo-cho, 790-8577 Matsuyama, Japan
[b] Department of Earth and Planetary Systems Science, Hiroshima University, Higashi-Hiroshima, 739-8526 Hiroshima, Japan
[c] Hiroshima Institute of Plate Convergence Region Research (HiPeR), Hiroshima University, Higashi-Hiroshima, 739-8526 Hiroshima, Japan

ARTICLE INFO

Article history:
Received 21 March 2018
Accepted after revision 23 September 2018
Available online 17 December 2018

Keywords:
Chlorite
23-Å phase
MASH
Hydrous phase
Subduction zone

ABSTRACT

A series of experiments was conducted on the decomposition of natural and chemically mixed chlorites to examine the stable hydrous phases in the MgO–FeO–Al_2O_3–SiO_2–H_2O (MFASH) system under 5–12 GPa and 700–1100 °C. The upper pressure and temperature limits of the stability region of chlorite are consistent with those observed in previous studies. The hydrous aluminum bearing pyroxene (phase HAPY) and Mg-sursassite (Sur) were observed just above the temperature stability region of chlorite (Chl); clinohumite (cHm) was observed coexisting with phase HAPY at 6 GPa and 800 °C and coexisting with the 23-Å phase at 7 GPa and 800 °C, which may suggest the transportation of water through Chl → (HAPY → cHm) → 23-Å phase along a relatively warm slab. The 23-Å phase has a wider stability region in the pure MASH system (up to 12 GPa and 1100 °C) than it does in the MFASH system (7–10 GPa, up to 1000 °C). The stability of the 23-Å phase beyond the chlorite breakdown pressure indicates that it may play an important role in transporting water into the deep Earth and even into the mantle transition zone.

1. Introduction

Antigorite (Atg) and chlorite (Chl) are believed to be the dominant hydrous phases in the shallow parts of the hydrated ultramafic lithosphere (e.g., Grove et al., 2006; Iwamori, 1998, 2007; Pawley, 2003; Rüpke et al., 2004; Schmidt and Poli, 1998). In natural peridotite, aluminum can extend the stability region of antigorite to much higher pressure and temperature (e.g., Bromiley and Pawley, 2003). On the other hand, in a higher-Al region which has about 5 wt% of Al_2O_3 component, approximately 15 wt% chlorite can form, which is stable at higher temperatures and pressures than antigorite (Grove et al., 2012). The reaction antigorite = forsterite + clinoenstatite + chlorite + water will allow up to 40% of its original water in antigorite to be preserved in chlorite, which may greatly increase the thermal stability of the hydrous phases in an Al-bearing system.

However, it appears that a depth of ~200 km represents the upper limit at which water can be preserved in normal subduction slabs, as previous studies have shown that most water will gradually be lost after the breakdown of chlorite and antigorite when reaching this depth (e.g., Fumagalli and Poli, 2005; Poli and Schmidt, 2002; Schmidt and Poli, 1998). The dehydration of chlorite or antigorite is

* Corresponding author at: Stony Brook University, 130 Earth and Space Sciences Building, 11794-2100 Stony Brook, NY, USA.
E-mail address: nao.cai@stonybrook.edu (N. Cai).

https://doi.org/10.1016/j.crte.2018.09.010
1631-0713/

believed to have some relation to the double seismic zone (e.g., Fumagalli and Poli, 2005; Mainprice and Ildefonse, 2009). Many previous experiments have only focused on the dehydration/decomposition boundary of chlorite (e.g., Fawcett and Yoder, 1966; Fockenberg, 1995; Fumagalli et al., 2014; Staudigel and Schreyer, 1977; Trommsdorff, 1999), which revealed that only small amounts of water could be preserved in Mg-sursassite along very cold subduction zones. However, phase relations in the pure chlorite system has not been examined so far at pressures higher than 7 GPa.

Recently several Al-bearing hydrous phases were found beyond the stability of chlorite, such as the hydrous Al-bearing pyroxene called HAPY phase [$Mg_{2.1}Al_{1.8}Si_{1.1}O_6(OH)_2$, Gemmi et al. (2011)], the 11.5-Å phase [$Mg_6Al(SiO_4)_2(OH)_7$, Gemmi et al. (2016)] and HySo phase [$Mg_3Al(Si_2O_7)(OH)_3$, Gemmi et al. (2016)]. The stabilities of these hydrous silicates may represent possible ways for water to enter the deep mantle at depths of more than 150 km. The formation of HAPY phase was given by: chlorite = phase-HAPY + fosterite + pyrope + H_2O at temperatures higher than 700 °C at ~5.4 GPa; Gemmi et al. (2011) also predicted the coexistence of phase HAPY and Mg-sursassite at lower temperatures.

In addition, we also reported a new Al-bearing hydrous phase named the 23-Å phase (Cai et al., 2015) after its characteristic *c*-axis. We observed the coexistence of the 23-Å phase and phase HAPY at 7 GPa and 800 °C using the bulk composition of $Mg_{11}Al_2Si_4O_{16}(OH)_{12}$ as the starting material. Only the 23-Å phase was observed at higher pressures and temperatures, which may suggest the transportation of water via chlorite → phase HAPY (+ sursassite) → 23-Å phase with increasing pressure.

The findings of these previously unknown hydrous phases may indicate that water release and transportation processes in the MASH system are more complex than in the MSH system. Thus, it is important to reconstruct the phase assemblages in Al-bearing systems. In such systems, chlorite is the predominant hydrous phase in the lower *P–T* regions, and it may be largely distributed in some local regions related to subduction zones (e.g., Bebout, 2007; Marschall and Schumacher, 2012; Spandler et al., 2008). Chlorite should be a very suitable starting material to examine the decomposition or dehydration of Al-bearing subduction zones to clarify whether water can be preserved and how much water can be transported into the deep mantle in the form of the 23-Å phase and other hydrous phases.

In a preliminary experiment under 10 GPa and 1000 °C using natural chlorite as the starting material, the 23-Å phase was found to coexist with pyrope, chondrodite, and phase A, with small amounts of fluid. In this study, we will further examine the decomposition of chlorite at conditions beyond the stability region of chlorite.

2. Experimental procedures

High-pressure and high-temperature experiments were conducted at the Geodynamics Research Center, Ehime University, using a Kawai-type 2000-ton multi-anvil apparatus. Tungsten carbide cubes with a truncated edge length of 8 mm and a Co-doped MgO octahedron with an edge length of 14 mm were adopted as the second-stage anvils and pressure medium, respectively. Pressure calibration was performed at room temperature, using the phase transitions Bi I–II, Bi III–V, and ZnS at 2.55, 7.7, and 15.6 GPa, respectively. Furthermore, the coesite–stishovite transitions (Ono et al., 2017) at 900 °C and 1300 °C were used to evaluate pressures at high temperatures; these experiments confirmed that there was no significant difference (within 0.5 GPa) between the pressures at room temperature and high temperatures of 900 °C and 1300 °C. Thus, the pressure uncertainties were assumed to be ±0.5 GPa. A cylindrical graphite sleeve was used as the heater. The temperature was monitored using a $W_{97}Re_3$–$W_{75}Re_{25}$ thermocouple and was controlled within ±5 °C.

The starting materials were a natural sample that comprises almost pure chlorite (from Russia, named ChlN), with a composition of $(Mg_{5.0}Fe_{0.2}Al_{0.8})(Al_{0.8}Si_{3.2})O_{10}(OH)_8$, and a chemical mixture of oxides (ChlM) with the composition of clinochlore [$Mg_5Al_2Si_3O_{10}(OH)_8$]. The compositions are listed in Table 1 and plotted in Fig. 1. The natural chlorite contains approximately 2.5 wt% FeO_T (T refers to ferric or ferrous iron) and approximately 14 wt% Al_2O_3, which is ~4 wt% less than that in ChlM. All the iron was counted as Fe^{2+} in the EPMA analyses. All of the starting materials were crushed to a grain size of less than 1 μm and preserved in a drying oven. No extra water was added to the starting materials, except for absorbed water, which was believed to be negligible.

A microfocused X-ray diffractometer (Cu Kα radiation, RIGAKU, RAPIDII-V/DW) operated at 40 kV and 15 mA was

Table 1
Chemical compositions of starting materials.

	MgO	Al_2O_3	SiO_2	FeO_T	H_2O	Total
ChlN[a]	35.5	14.4	33.8	2.5	12.8[c]	99.0
ChlM[b]	36.3	18.3	32.4	0	13.0	100

[a] Measured by EPMA with WDS.
[b] Weighted values of the oxides.
[c] Calculated value from the structural formula.

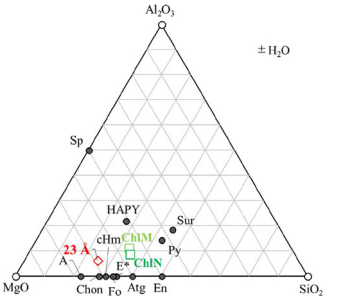

Fig. 1. Chemical compositions (in moles) of the starting materials (green squares) and possible mantle minerals shown in the Mg–Al–Si ternary diagram. The iron content is added into the MgO component in this ternary diagram, thus olivine is expressed as forsterite here and after. The symbol * marks the nonstoichiometric phase E. A: phase A; E: phase E; En: enstatite; Fo: forsterite; Sp: spinel; Atg: antigorite; Py: pyrope; Sur: Mg-sursassite; cHm: clinohumite; Chon: chondrodite; HAPY: hydrous Al-bearing pyroxene; 23 Å: 23-Å phase.

used to identify the phases in the run products. The chemical compositions of those mineral phases, including the starting material of the natural chlorite sample, were measured using a wave-dispersive electron probe micro-analyzer (WDS EPMA, JEOL JXA 8800) and energy-dispersive spectroscopy in a scanning electron microscope (EDS SEM, JEOL JSM-6510LV, with an accelerating voltage of 15 kV). Standards of known composition, including natural and synthesized forsterite and enstatite for Mg, Si and Fe, kyanite for Al, and wollastonite for Ca, were used in the measurements. The EPMA was operated at accelerating voltage of 15 kV and beam current of 10 nA, with a beam size of 1–2 μm.

In the run products, equilibrium was judged by grain growth and the coexisting phases in the system, combined with the absence of fluid inclusions in the grains, based on the discussion of Fumagalli et al. (2014). In some experiments, however, inclusions and zonation can be identified in some grains. In these cases, mass balance calculations and chemographies were used to describe the equilibrium phase assemblages.

3. Results and discussion

Before we discuss the experimental results, we must correct the formula of the 23-Å phase reported by Cai et al. (2015). The preliminary results of the single-crystal X-ray analysis suggest that the reasonable oxygen number in a unit cell of the 23-Å phase should be 30 instead of 28, as was assumed by Cai et al. (2015). A recent study of a new hydrous phase (the 11.5-Å phase, $Mg_6Al(OH)_7(SiO_4)_2$) by Gemmi et al. (2016), which has a similar chemical composition, crystal structure and even compressibility as the 23-Å phase (Cai et al., 2015), indicates that they may be the same phase, or very similar to each other. By examining the WDS and EDS results of the 23-Å phase, especially for those obtained at relatively higher pressures and temperatures (which should be more in equilibrium than the lower ones), the ideal formula of the 23-Å phase is corrected to be $Mg_{12}Al_2Si_4O_{16}(OH)_{14}$, with a calculated density of 2.941 g/cm^3 and a water content of 13.2 wt%. In addition, we measured the density of a bulk sample (2.947 g/cm^3) mostly containing the 23-Å phase with approximately 5 vol% pyrope using Archimedes' method. The determined density of the pure 23-Å phase is ~2.911 g/cm^3, which is close to the value (2.93 g/cm^3) reported by Gemmi et al. (2016).

The high-pressure and high-temperature experiments were conducted at 5–12 GPa and 700–1100 °C for natural chlorite (ChlN) and 8–11 GPa and 1000–1100 °C for the chemical-mixed clinochlore composition (ChlM). The experimental conditions, run products, and representative WDS & EDS results of the chemical compositions of the run products are summarized in Table 2 and Tables SM1 and SM2. Fig. 2 shows some backscattered electron images of the run products in the natural chlorite (MFASH) system. Although the temperature gradient within the capsule should be small (less than 50 °C), some run products show slightly different phase assemblages at different temperature zones.

3.1. Decomposition of chlorite

Detailed reviews of the phase relations in the MASH system concerning chlorite were made by Trommsdorff (1999) and Fumagalli et al. (2014). Four invariant points were discussed, involving the phases of forsterite, enstatite, spinel, pyrope, diaspore/corundum, and hydrous phases of chlorite and Mg-sursassite. Chlorite was totally dehydrated at low pressures (2–5 GPa) and high temperatures (900–750 °C) in the garnet stability field by the following reaction:

$$\text{chlorite} = \text{forsterite} + \text{pyrope} + \text{spinel} + H_2O \quad \text{(Fockenberg, 1995; Staudigel and Schreyer, 1977)}, \quad (1)$$

while at higher pressures and lower temperatures, Mg-sursassite formed as a hydrous product after the breakdown of chlorite by the following reaction:

Table 2
Experimental conditions and run products.

Run#	*P*/GPa	*T*/°C	*T*/h	Starting composition	Results
ChlN1	5	800	6	ChlN	Py + Ol + Sp + F
ChlN2	6	700	6	ChlN	Ol + Chl + Sur + Sp + F
ChlN3	6	800	6	ChlN	Py + Ol + HAPY + F; Py + Ol + Sp + F; Py + cHm + Sp + F
ChlN4	7	700	6	ChlN	Ol + Sur + 23-Å + F; cHm + Sur + 23-Å + F
ChlN5	7	800	4	ChlN	Py +23-Å + Ol + F; Py + 23-Å + cHm + F
ChlN6	8	700	6	ChlN	Py + 23-Å + Chon + Chl
ChlN7	8	1000	2	ChlN	Py + Chon + Br + F
ChlN9	10	1000	8	ChlN	Py + 23-Å + Chon + F; Py + 23-Å + A + F
ChlN10	10	1000	3	ChlN	Py + 23-Å + Chon + F
ChlN11	11	1000	2	ChlN	Py + A + Al-E + F
ChlN12	11	1100	4	ChlN	Py + Chon + Br+ F; Py + A + F; Py + Al-E + F
ChlN13	12	1000	8	ChlN	Py + Al-E + Br + F
ChlM1	8	1000	2	ChlM	Py + Chon + Sp + F; Py + 23-Å + Sp + F
ChlM2	11	1000	2	ChlM	Py + 23-Å + Al-? + F
ChlM3	11	1100	4	ChlM	Py + 23-Å + Al-? + F

ChlN: natural chlorite, ChlM: chemical mixture with the same composition as that of clinochlore; Py: pyrope garnet; Ol: olivine; Sp: spinel; cHm: clinohumite; Br: brucite; F: fluid; Chl: chlorite; Sur: sursassite; HAPY: hydrous Al-bearing pyroxene; 23-Å: 23-Å phase; Chon: chondrodite; A: phase A; Al-E: Al-bearing phase E; Al-?: Al-bearing unknown phase. The fluid was identified at the occurrence of bubbles when opening the capsules, in conjunction with the porosity after polishing the entire charge for the SEM measurements.

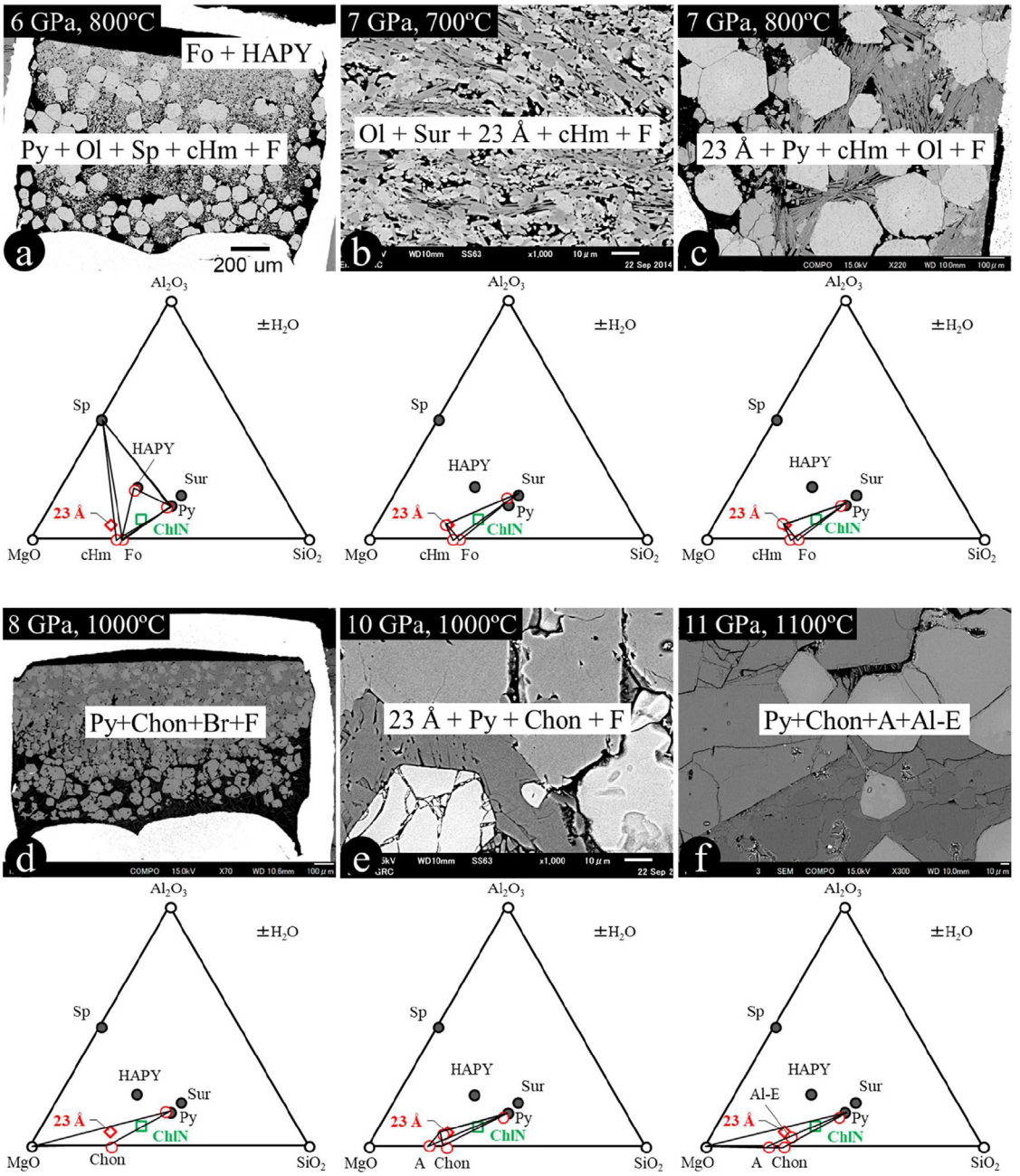

Fig. 2. Back-scattered electron images of selected run products and the phase coexistences in the ternary $MgO–SiO_2–Al_2O_3$ system using natural chlorite as the starting material. See text for detailed discussion. A: phase A; Al-E: aluminum-bearing phase E; Ol: olivine; Sp: spinel; Py: pyrope; Chl: chlorite (clinochlore); Sur: Mg-sursassite; cHm: clinohumite; Chon: chondrodite; HAPY: hydrous Al-bearing pyroxene; 23-Å: 23-Å phase.

chlorite = forsterite + Mg-sursassite + diaspore + H_2O (Fockenberg, 1995). (2)

In the present study, the above decomposition reactions (1) and (2) were successfully constrained, which was consistent with the results of previous studies (see the thin solid and dashed lines in Fig. 3). Chlorite was found to totally dehydrate into pyrope, olivine, spinel, and fluid above 800 °C at 5 GPa, while it decomposed into olivine, Mg-sursassite and fluid at 6 GPa and 700 °C. The reason why we did not observe diaspore in the present experiment may be due to slight compositional differences between current chlorite (low Al content) and the previous ones (e.g., Fockenberg, 1995; Fumagalli et al., 2014).

In addition, phase HAPY was found to mostly coexist with pyrope, olivine, and fluid in the low-temperature portion of the run at 6 GPa and 800 °C (upper portion of Fig. 2a), which may imply a very narrow stability region for the phase HAPY above the stability of chlorite. The reaction

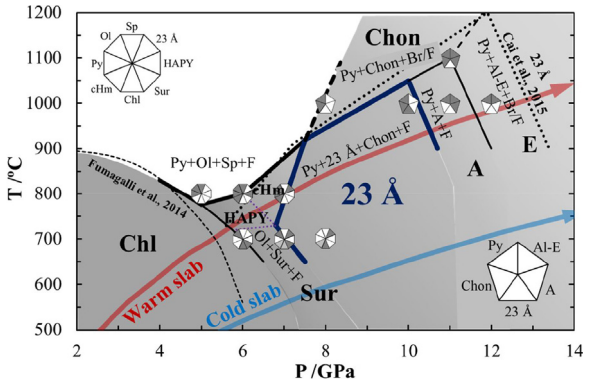

Fig. 3. Stability of hydrous phases in chlorite composition. Our recovered phase assemblages are also shown. Typical warm and cold slab geotherms are from Kirby et al. (1996). The tick dark blue line indicates the stability region of the 23-Å phase in the composition of chlorite. The thick black line indicates the total dehydration boundary. The dotted line indicates the stability region of the 23-Å phase in the Fe-free pure 23-Å phase composition (Cai et al., 2015). Chl: chlorite; HAPY: hydrous Al-bearing pyroxene; cHm: clinohumite; Sur: Mg-sursassite; 23-Å: 23-Å phase; A: phase A; E: phase E; Al-E: Al-bearing phase E; Chon: chondrodite; Py: pyrope; Ol: olivine; Sp: spinel; F: fluid; Br: brucite.

is given by:

$$13\text{chlorite} = 16\text{olivine} + 4\text{pyrope} + 10\text{phase-HAPY} + 42H_2O, \quad (3)$$

which was constrained by Gemmi et al. (2011).

3.2. Phase HAPY and clinohumite

At 6 GPa and 800 °C, pyrope, olivine and spinel were found to coexist with clinohumite and fluid, while phase HAPY was mostly found in the low-temperature zone, which may imply an invariant point near such conditions, with three possible reactions, i.e. reactions (1) and (3) and the following reaction (4):

$$20\text{phase-HAPY} = 7\text{olivine} + 5\text{pyrope} + 13\text{spinel} + 20H_2O \quad (\text{Fumagallietal.}, 2014). \quad (4)$$

The results obtained here indicate that the stability region of the phase HAPY occurs at slightly higher temperatures and pressures than that of Fumagalli et al. (2014). This minor difference may arise from differences in the bulk composition (e.g., Cr content).

The formation of clinohumite beyond the stability of phase HAPY is controlled by the following reaction:

$$10\text{phase-HAPY} + 120\text{olivine} + 16H_2O = 9\text{pyrope} + 26\text{clinohumite}, \quad (5)$$

at 6-7 GPa and ~800 °C.

In the present study, we did not observe the coexistence of phase HAPY and Mg-sursassite (Gemmi et al., 2011), which may also be due to differences in bulk composition. The chemical composition of phase HAPY observed at 6 GPa and 800 °C corresponds to the formula $Mg_{2.15}Fe_{0.05}Al_{1.73}Si_{1.1}O_6(OH)_2$; it is enriched in Mg (in the form of Mg plus Fe) and lower in Al compared with that of Gemmi et al. (2011).

In addition, the run product obtained at 7 GPa and 800 °C shows the coexistence of pyrope, olivine, clinohumite and the 23-Å phase, plus fluid, which implies that the reaction from a clinohumite-bearing phase assemblage to a 23-Å phase-bearing phase assemblage occurs with increasing pressure.

3.3. Formation of the 23-Å phase

The present results indicate that the lowest pressure at which the 23-Å phase can be formed is ~7 GPa. This 23-Å phase coexists with olivine, Mg-sursassite, and a small amount of fluid at 700 °C (Fig. 2b) while it coexists with pyrope, olivine, clinohumite, and fluid at 800 °C (Fig. 2c). The formation of the 23-Å phase can be given by reactions (6) and (7):

$$\text{olivine} + \text{diaspore} + H_2O = \text{Mg-sursassite} + \text{23-Åphase}(\text{atlowpressure}) \quad (6)$$

$$\text{olivine} + \text{Mg-sursassite} = \text{pyrope} + \text{23-Åphase} + H_2O(\text{athighpressure}) \quad (7)$$

at low temperature, while its formation at higher temperatures occurs through the following reaction:

$$\text{clinohumite} + \text{HAPY} + H_2O = \text{pyrope} + \text{23-Åphase} \quad (8)$$

With increasing pressure, clinohumite will be further consumed by the following reaction:

$$\text{clinohumite} + \text{23-Å} = \text{pyrope} + \text{chondrodite} \quad (9)$$

The first detailed report on the 23-Å phase was given by Cai et al. (2015), who revealed its stability region in the *P–T* range of 6–12 GPa and 700–1200 °C. However, an unknown hydrous phase, called the 11.5-Å phase, was observed by Fumagalli et al. (2014) in the Cr_2O_3–MgO–Al_2O_3–SiO_2–H_2O system at 6 GPa, 650 °C and 6.5 GPa, 700 °C, which may be the same as the 23-Å phase. The 11.5-Å phase has Mg:Al:Si ratio and XRD pattern similar to those of the 23-Å phase. However, there are no data about the 11.5-Å phase at higher pressures and temperatures. In addition, at higher concentrations of Cr_2O_3, no 11.5-Å phase was observed at 6 GPa and 750 °C, which may suggest that Cr decreases the stability of the 11.5-Å phase.

3.4. Decomposition of the 23-Å phase and water transfer to the deep mantle

In this study, the 23-Å phase is stable up to 10 GPa and 1000 °C (MFASH system); then, it decomposes to chondrodite, phase A and/or Al-bearing phase E at higher temperatures or pressures. Above the stability of the 23-Å phase, chondrodite was found to coexist with pyrope and fluid at 8–10 GPa, while phase A coexisted with pyrope,

small amounts of Al-bearing phase E, and some fluids at 11 GPa and 1000 °C and with pyrope, chondrodite, Al-bearing phase E and fluid at 1100 °C (Fig. 2f). Only a negligible amount of aluminum ($Al_2O_3 < 0.4$ wt%) was observed in phase A. The reactions concerning chondrodite are given by the following reactions (Fig. 2d–e):

$$\text{23-Åphase} + \text{chondrodite} = \text{phaseA} + \text{pyrope} + \text{F(atlowertemperature)} \quad (10)$$

$$\text{23-Åphase} = \text{pyrope} + \text{chondrodite} + \text{brucite} + \text{F(athighertemperature)} \quad (11)$$

At 12 GPa and 1000 °C, only pyrope and the Al-bearing phase E were observed, without or with the release of very little water. The reaction from a phase A- to a phase E-bearing phase assemblage can be given by the following reactions:

$$\text{pyrope} + \text{phaseA} + H_2O = \text{Al-bearingphaseE}; \quad (12)$$

$$\text{phaseA} = \text{phaseE} + \text{periclase/brucite}. \quad (13)$$

At higher temperatures, phase A or Al-bearing phase E will decompose to chondrodite and brucite or pyrope, chondrodite and fluid by the following reaction:

$$\text{phaseA} = \text{chondrodite} + 2\text{brucite} \quad (14)$$

$$\text{Al-bearingphaseE} = \text{pyrope} + \text{chondrodite} + H_2O \quad (15)$$

Phase E is stable up to 17 GPa and 1100 °C in the MSH system (e.g., Komabayashi and Omori, 2006); then, it will decompose to superhydrous phase B. As aluminum may stabilize hydrous phases at higher temperatures [e.g., antigorite, Bromiley and Pawley (2003)], the Al-bearing phase E should have a wide stability region. Thus, the reaction of the 23-Å phase to form phase A and phase E with increasing pressure may allow almost the same amount of water to be preserved in the slabs and then subducted to the mantle transition zone.

3.5. The effect of Fe or Al on the stability of the 23-Å phase

We conducted some additional experiments at 8 and 11 GPa and 1000 and 1100 °C to examine the effect of aluminum or iron on the stability of the 23-Å phase, using chemical-mixed oxides with clinochlore composition (ChlM) as the starting material. Some backscattered electron images of the run products are shown in Fig. 4; the results are listed in Table SM1 and summarized in Fig. 5.

The 23-Å phase has a larger stability region in the pure MASH system than it does in the MFASH system, by ~50 °C and ~2 GPa of temperature and pressure, respectively. Note that ChlM is iron-free and contains ~4 wt% more Al than ChlN. The high Al content in the 23-Å phase suggests that the 23-Å phase tends to be stable in the Al-bearing system. Thus, our results may indicate that the aluminum content in the bulk composition could extend the stability region of the 23-Å phase to higher pressures and temperatures, as is shown in the case of antigorite (e.g., Bromiley and Pawley, 2003). Further experiments will be

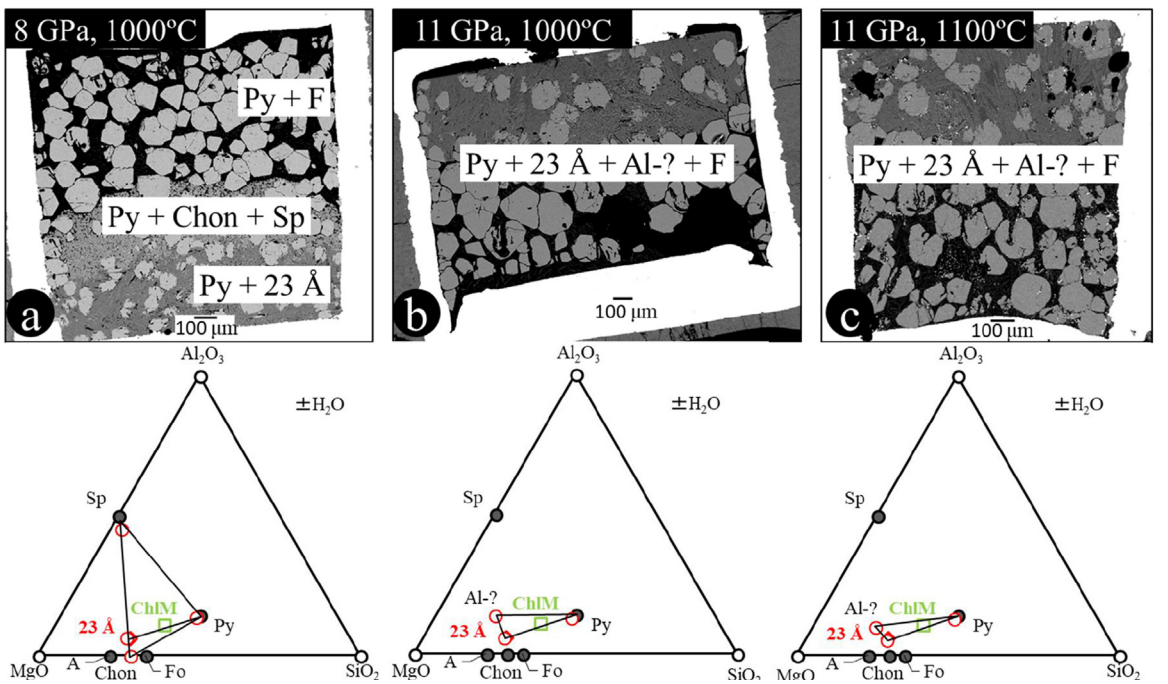

Fig. 4. Top: back-scattered electron images of selected run products using clinochlore (ChlM) as the starting material. Bottom: compositional triangles in the $MgO–SiO_2–Al_2O_3$ system showing the equilibrium phase assemblages, respectively. Open circles are the measured compositions of the run products. Py: pyrope; 23-Å: 23-Å phase; Chon: chondrodite; Sp: spinel; A: phase A; Fo: forsterite; F: fluid; Al-?: Al-bearing unknown phase.

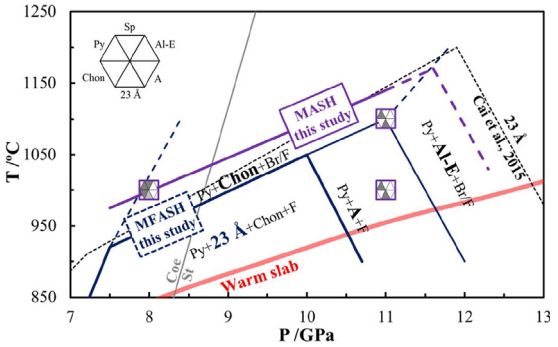

Fig. 5. Stability of the 23-Å phase in MASH system (clinochlore composition, purple line) compared with that in MFASH (natural chlorite) system (blue lines from Fig. 3). Py: pyrope; 23-Å: 23-Å phase; Chon: chondrodite; Sp: spinel; F: fluid; A: phase A; Al-E: Al-bearing phase E; Br: brucite. The Coe/St phase boundary is from Zhang et al. (1996). The dotted line indicates the stability region of the 23-Å phase from Cai et al., 2015.

conducted to precisely determine the effects of other components (e.g., iron, aluminum, chromium) on the stability of the 23-Å phase and other hydrous phases in the MASH system.

4. Implications for the Earth's interior

The discovery of phase HAPY and the 23-Å phase above the stability of chlorite is important for considering the thermal stability region of hydrous phases in Al-bearing subduction zones. As antigorite cannot hold large amounts of aluminum [up to 5 wt%, e.g., Padrón-Navarta et al., 2013; Wicks and O'Hanley,1988], chlorite should be stabilized in an Al-bearing system related to a subduction zone, as indicated by Marschall and Schumacher (2012) and Spandler et al. (2008). For example, fertile peridotite has enough Al_2O_3 to stabilize 6–7 wt% chlorite (Grove et al., 2012). Thus, the results of the present study indicate that the dehydration position and water transportation mechanism in the slabs of Al-bearing systems must be modified.

4.1. "Choke point" in an Al-bearing slab

The "choke point" (Kawamoto et al., 1996) in the MSH system was constrained by the decomposition of antigorite and the dehydration of phase A. Previous results have shown that total dehydration occurs at approximately 550 °C at 5 GPa (e.g., Komabayashi and Omori, 2006; Komabayashi et al., 2005; Ulmer and Trommsdorff, 1995). Since Al stabilizes antigorite and chlorite to higher temperatures (e.g., Bromiley and Pawley, 2003), the dehydration boundaries in Al-bearing systems extend to higher temperatures.

In addition, the presence of phase HAPY, and especially that of the 23-Å phase, greatly extends the thermal stability of hydrous phases in Al-bearing systems, as the present study shows that the total dehydration of chlorite occurs at approximately 800 °C at 5 GPa in the MFASH system, which is ~250 °C higher than that in the MSH system. In addition, Al-bearing antigorite decomposes to a chlorite-bearing assemblage prior to total dehydration (Bromiley and Pawley, 2003). Thus, even in a relatively warm slab, a significant volume of water can be preserved in the form of chlorite, and then as phase HAPY-, clinohumite-, and 23-Å phase-bearing assemblages into the deeper parts of the upper mantle.

4.2. Water transportation mechanism along an Al-bearing subducting slab

During the decomposition of Al-bearing antigorite to chlorite and that of chlorite to HAPY/cHm, some water should be released at 5–7 GPa and 600–800 °C. Considering the upper layer of a subduction zone, which comprises metamorphosed MORB (e.g., Poli and Schmidt, 2002), the released H_2O fluid from the lower peridotite layer should be absorbed into the MORB composition, and lawsonite forms (e.g., Okamoto and Maruyama, 1999; Schmidt and Poli, 1998). Lawsonite has a wide stability region up to 8 GPa and 800 °C and a high aluminum content that can promote the formation of chlorite, the 23-Å phase or other Al-bearing hydrous phases at slab–mantle wedge interaction zones. In our pressure and temperature range, we did not observe the 10-Å phase in our experiments, which may suggest that the 10-Å phase is not stable in aluminum-bearing systems. Therefore, the 10-Å phase is omitted from our following discussion.

Based on the present study, a hypothesis (Fig. 6) could be made that, in a relatively warm and Al-bearing slab, water is transferred from chlorite to phase HAPY and clinohumite at ~200 km. At depths of more than 200 km, water could be preserved in the form of the 23-Å phase and/or phase A and then transferred to the deeper parts of the upper mantle. The coexistence of the 23-Å phase and phase A depends on the aluminum content of the bulk composition of the subducting slabs.

Two main dehydration positions are included in this hypothesis. One position is related to the dehydration or decomposition of antigorite at a depth of approximately 120 km (~ 4 GPa). At this position, at least 70 wt% of its water could be released out into the upper MORB layer and mantle wedge (Schmidt and Poli, 1998). Because of the

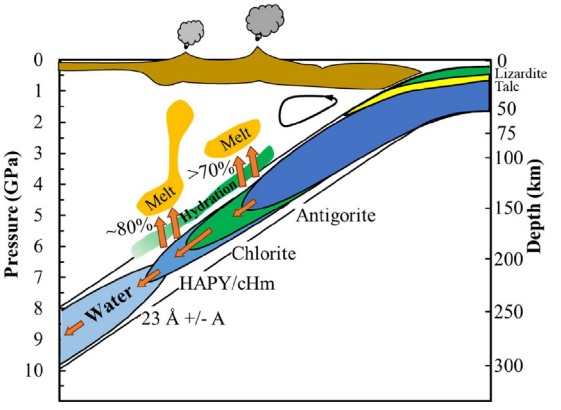

Fig. 6. Hypothesis for water transportation in a relatively warm (Fig. 3) and Al-bearing subduction zone. This figure is modified from Fumagalli and Poli (2005).

high aluminum content at the shallow sediment layer of the subducting slab, some amount of water would cause the hydration of the mantle wedge to form chlorite-bearing rocks (because chlorite has a higher temperature stability than antigorite or other hydrous phases). Such chlorite-bearing rocks could be dragged by the descending slab, thus transferring water to depths of more than 120 km. There is still a large amount of fluid that could further rise and induce partial melting of the mantle wedge to form magma.

The other position is related to the dehydration or decomposition of chlorite at approximately 200 km (~6 GPa). During dehydration, approximately 80 wt% of its water would be lost to the upper MORB layer and mantle wedge, which could induce the hydration and partial melting of the mantle wedge. Based on our results, the further descending of this slab could lead to the phase transformation from chlorite to phase HAPY and/or clinohumite, then to the 23-Å phase and/or phase A. Up to 20% of its original water would be preserved in those hydrous phases and then be transferred to depths as great as the mantle transition zone.

These two dehydration positions could be the reason for the development of two main volcanic zones that are parallel to each other and the trench (e.g., Tatsumi and Eggins, 1995), such as the Northeast Japan Arc.

5. Conclusions

Decomposition experiments of chlorite were conducted in this study. Rather than observing total dehydration, we observed several hydrous phases above the stability region of chlorite at relatively high temperatures, such as phase HAPY, clinohumite and the 23-Å phase. At higher pressures, phase A, Al-bearing phase E and chondrodite are the stable hydrous phases. These results indicate that up to 20% of its original water could be preserved in those hydrous phases, even in a relatively warm slab. Thus, water could be transported into the deep upper mantle in Al-bearing subduction zones and even transported into the deep transition zone by the 23-Å phase, phase, A and Al-bearing phase E.

Acknowledgment

This work was conducted as a part of the PhD thesis of N. Cai at Ehime University. The authors would like to thank T. Shinmei and H. Ohfuji for their help with high-pressure experiments and quantitative measurements. This work was supported by a Grant-in-Aid for Scientific Research (A) [KAKENHI] from the Japan Society for the Promotion of Science (JSPS) given to T. Inoue (No. 26247073).

Appendix A. Supplementary data

Supplementary data associated with this article can be found, in the online version, at https://doi.org/10.1016/j.crte.2018.09.010.

References

Bebout, G.E., 2007. Metamorphic chemical geodynamics of subduction zones. Earth Planet. Sci. Lett. 260, 373–393.
Bromiley, G.D., Pawley, A.R., 2003. The stability of antigorite in the systems $MgO–SiO_2–H_2O$ (MSH) and $MgO–Al_2O_3–SiO_2–H_2O$ (MASH): The effects of Al^{3+} substitution on high-pressure stability. Am. Mineral. 88, 99–108.
Cai, N., Inoue, T., Fujino, K., Ohfuji, H., Yurimoto, H., 2015. A possible new Al-bearing hydrous Mg-silicate (23 angstrom phase) in the deep upper mantle. Am. Mineral. 100, 2330–2335.
Fawcett, J., Yoder, H., 1966. Phase relationships of chlorites in the system $MgO–Al_2O_3–SiO_2–H_2O$. Am. Mineral. 51, 353.
Fockenberg, T., 1995. New experimental results up to 100 kbar in the system $MgOAl_2O_3$-SiO_2-H_2O (MASH): Preliminary stability fields of chlorite, chloritoid, staurolite, MgMgAl-pumpellyite, and pyrope. Bochumer Geologischeand Geotechnische Arbeiten 44, 39–44.
Fumagalli, P., Poli, S., 2005. Experimentally determined phase relations in hydrous peridotites to 6.5 GPa and their consequences on the dynamics of subduction zones. J. Petrol. 46, 555–578.
Fumagalli, P., Poli, S., Fischer, J., Merlini, M., Gemmi, M., 2014. The high-pressure stability of chlorite and other hydrates in subduction melanges: experiments in the system $Cr_2O_3–MgO–Al_2O_3–SiO_2–H_2O$. Contrib. Mineral. Petrol. 167, 979.
Gemmi, M., Fischer, J., Merlini, M., Poli, S., Fumagalli, P., Mugnaioli, E., Kolb, U., 2011. A new hydrous Al-bearing pyroxene as a water carrier in subduction zones. Earth Planet. Sci. Lett. 310, 422–428.
Gemmi, M., Merlini, M., Palatinus, L., Fumagalli, P., Hanfland, M., 2016. Electron diffraction determination of 11.5 Å and HySo structures: Candidate water carriers to the Upper Mantle. Am. Mineral. 101, 2645–2654.
Grove, T.L., Chatterjee, N., Parman, S.W., Médard, E., 2006. The influence of H_2O on mantle wedge melting. Earth Planet. Sci. Lett. 249, 74–89.
Grove, T.L., Till, C.B., Krawczynski, M.J., 2012. The Role of H_2O in Subduction Zone Magmatism. Annu. Rev. Earth Planet. Sci. 40, 413–439.
Iwamori, H., 1998. Transportation of H_2O and melting in subduction zones. Earth Planet. Sci. Lett. 160, 65–80.
Iwamori, H., 2007. Transportation of H_2O beneath the Japan arcs and its implications for global water circulation. Chem. Geol. 239, 182–198.
Kawamoto, T., Hervig, R.L., Holloway, J.R., 1996. Experimental evidence for a hydrous transition zone in the early Earth's mantle. Earth Planet. Sci. Lett. 142, 587–592.
Kirby, S.H., Stein, S., Okal, E.A., Rubie, D.C., 1996. Metastable mantle phase transformations and deep earthquakes in subducting oceanic lithosphere. Rev. Geophys. 34, 261–306.
Komabayashi, T., Hirose, K., Funakoshi, K.-I., Takafuji, N., 2005. Stability of phase A in antigorite (serpentine) composition determined by in situ X-ray pressure observations. Phys. Earth Planet. Inter. 151, 276–289.
Komabayashi, T., Omori, S., 2006. Internally consistent thermodynamic data set for dense hydrous magnesium silicates up to 35 GPa, 1600C: implications for water circulation in the Earth's deep mantle. Phys. Earth Planet. Inter. 156, 89–107.
Mainprice, D., Ildefonse, B., 2009. Seismic anisotropy of subduction zone minerals–contribution of hydrous phases. Subduction zone geodynamics. Springer, 63–84.
Marschall, H.R., Schumacher, J.C., 2012. Arc magmas sourced from mélange diapirs in subduction zones. Nat. Geosci. 5, 862–867.
Okamoto, K., Maruyama, S., 1999. The high-pressure synthesis of lawsonite in the MORB + H_2O system. Am. Mineral. 84, 362–373.
Ono, S., Kikegawa, T., Higo, Y., Tange, Y., 2017. Precise determination of the phase boundary between coesite and stishovite in SiO_2. Phys. Earth Planet. Inter. 264, 1–6.
Padrón-Navarta, J.A., Sánchez-Vizcaíno, V.L., Hermann, J., Connolly, J.A., Garrido, C.J., Gómez-Pugnaire, M.T., Marchesi, C., 2013. Tschermak's substitution in antigorite and consequences for phase relations and water liberation in high-grade serpentinites. Lithos 178, 186–196.
Pawley, A., 2003. Chlorite stability in mantle peridotite: the reaction clinochlore + enstatite = forsterite + pyrope + H_2O. Contrib. Mineral. Petrol. 144, 449–456.
Poli, S., Schmidt, M.W., 2002. Petrology of Subducted Slabs. Annu. Rev. Earth Planet. Sci. 30, 207–235.
Rüpke, L.H., Morgan, J.P., Hort, M., Connolly, J.A., 2004. Serpentine and the subduction zone water cycle. Earth Planet. Sci. Lett. 223, 17–34.
Schmidt, M.W., Poli, S., 1998. Experimentally based water budgets for dehydrating slabs and consequences for arc magma generation. Earth Planet. Sci. Lett. 163, 361–379.
Spandler, C., Hermann, J., Faure, K., Mavrogenes, J.A., Arculus, R.J., 2008. The importance of talc and chlorite "hybrid" rocks for volatile

recycling through subduction zones; evidence from the high-pressure subduction mélange of New Caledonia. Contrib. Mineral. Petrol. 155, 181–198.
Staudigel, H., Schreyer, W., 1977. The upper thermal stability of clinochlore, $Mg_5Al[AlSi_3O_{10}](OH)_8$, at 10–35 kb PH_2O. Contrib. Mineral. Petrol. 61, 187–198.
Tatsumi, Y., Eggins, S., 1995. Subduction zone magmatism. Wiley.
Trommsdorff, V., 1999. Phase relations of hydrous mantle subducting to 300 km. Mantle petrology: Field observations and high pressure experimentation. Geochemical Society, Washington DC259–282.
Ulmer, P., Trommsdorff, V., 1995. Serpentine stability to mantle depths and subduction-related magmatism. Science 268, 858–861.
Wicks, F., O'Hanley, D.S., 1988. Serpentine minerals; structures and petrology. Rev. Mineral. Geochem. 19, 91–167.
Zhang, J., Li, B., Utsumi, W., Liebermann, R.C., 1996. In situ X-ray observations of the coesite–stishovite transition: reversed phase boundary and kinetics. Phys. Chem. Miner. 23, 1–10.